

SIL1 mutations and clinical spectrum in patients with Marinesco-Sjögren syndrome

Michael Krieger,¹ Andreas Roos,² Claudia Stendel,³ Kristl G. Claeys,^{2,3} Fatma Mujgan Sonmez,⁴ Michael Baudis,^{5,6} Peter Bauer,⁷ Antje Bornemann,⁸ Christian de Goede,⁹ Andreas Dufke,⁷ Richard S. Finkel,¹⁰ Hans H. Goebel,¹¹ Martin Häussler,¹² Helen Kingston,¹³ Janbernd Kirschner,¹⁴ Livija Medne,¹⁵ Petra Muschke,¹⁶ François Rivier,^{17,18} Sabine Rudnik-Schöneborn,¹ Sabrina Spengler,¹ Francesca Inzana,¹⁹ Franco Stanzial,¹⁹ Francesco Benedicenti,¹⁹ Matthis Synofzik,^{20,21} Ana Lia Taratuto,²² Laura Pirra,²³ Stacey Kiat-Hong Tay,²⁴ Haluk Topaloglu,²⁵ Gökhan Uyanik,²⁶ Dorothea Wand,²⁷ Denise Williams,²⁸ Klaus Zerres,¹ Joachim Weis² and Jan Senderek²⁹

-
- 1 Institute of Human Genetics, Rheinisch-Westfälische Technische Hochschule (RWTH) Aachen University, 52074 Aachen, Germany
 - 2 Institute of Neuropathology and Jülich Aachen Research Alliance (JARA) Brain Translational Medicine, RWTH Aachen University, 52074 Aachen, Germany
 - 3 Department of Neurology and JARA Brain Translational Medicine, RWTH Aachen, 52074 Aachen University, Germany
 - 4 Department of Child Neurology, Turgut Ozal University Faculty of Medicine, Ankara 06510, Turkey
 - 5 Institute of Molecular Life Sciences, University of Zürich, 8057 Zürich, Switzerland
 - 6 Swiss Institute of Bioinformatics, 1015 Lausanne, Switzerland
 - 7 Institute of Medical Genetics and Applied Genomics, University of Tübingen, 72076 Tübingen, Germany
 - 8 Institute of Brain Research, University of Tübingen, 72076 Tübingen, Germany
 - 9 Department of Paediatric Neurology, Royal Preston Hospital, Lancashire PR2 9HT, UK
 - 10 Division of Neurology, Nemours Children's Hospital, Orlando, FL 32827, USA
 - 11 Department of Neuropathology, University Medical Centre of the Johannes Gutenberg University Mainz, 55131 Mainz, Germany
 - 12 Centre for Children with Developmental Disorders and Handicaps, Department of Paediatrics, University of Würzburg, 97080 Würzburg, Germany
 - 13 Genetic Medicine, Manchester Academic Health Sciences Centre, University of Manchester and Central Manchester University Hospitals NHS Foundation Trust, Manchester M13 9WL, UK
 - 14 Department of Paediatrics and Adolescent Medicine, Division of Neuropaediatrics and Muscle Disorders, University of Freiburg, 79106 Freiburg, Germany
 - 15 Division of Genetics, Department of Paediatrics, The Children's Hospital of Philadelphia, Philadelphia, PA 19104, USA
 - 16 Institute of Human Genetics, Otto-von-Guericke-University, 39120 Magdeburg, Germany
 - 17 CHRU Montpellier, Neuropédiatrie CR Maladies Neuromusculaires, 34295 Montpellier, France
 - 18 U1046, INSERM, Université Montpellier 1, Université Montpellier 2, 34295 Montpellier, France
 - 19 Department of Paediatrics, Genetic Counselling Service, Hospital of Bolzano, 39100 Bolzano, Italy
 - 20 Centre for Neurology and Hertie-Institute for Clinical Brain Research, University of Tübingen, 72076 Tübingen, Germany
 - 21 German Research Centre for Neurodegenerative Diseases (DZNE), 72076 Tübingen, Germany
 - 22 Department of Neuropathology, Institute for Neurological Research, FLENI, Buenos Aires, C1428AQK, Argentina
 - 23 Neurology Department, Favaloro Foundation, Buenos Aires, C1093AAS, Argentina
 - 24 Division of Paediatric Neurology and Developmental Paediatrics, National University of Singapore and National University Hospital, Singapore 119074, Singapore
 - 25 Department of Paediatric Neurology, Ihsan Dogramaci Children's Hospital, Ankara 06100, Turkey
 - 26 Centre for Medical Genetics, Hanusch Hospital, 1140 Vienna, Austria
 - 27 Department of Human Genetics and Medical Biology, University Hospital Halle, 06097 Halle, Germany
 - 28 West Midlands Regional Genetics Laboratories and the Department of Clinical Genetics, Birmingham Women's Foundation Trust, Edgbaston, Birmingham B15 2TG, UK
 - 29 Friedrich-Baur Institute, Department of Neurology, Ludwig-Maximilians University of Munich, 80336 Munich, Germany

Correspondence to: Dr. Jan Senderek,
Friedrich-Baur Institute,
Department of Neurology,
Ludwig-Maximilians University of Munich,
80336 Munich, Germany
E-mail: jan.senderek@med.uni-muenchen.de

Marinesco-Sjögren syndrome is a rare autosomal recessive multisystem disorder featuring cerebellar ataxia, early-onset cataracts, chronic myopathy, variable intellectual disability and delayed motor development. More recently, mutations in the *SIL1* gene, which encodes an endoplasmic reticulum resident co-chaperone, were identified as the main cause of Marinesco-Sjögren syndrome. Here we describe the results of *SIL1* mutation analysis in 62 patients presenting with early-onset ataxia, cataracts and myopathy or combinations of at least two of these. We obtained a mutation detection rate of 60% (15/25) among patients with the characteristic Marinesco-Sjögren syndrome triad (ataxia, cataracts, myopathy) whereas the detection rate in the group of patients with more variable phenotypic presentation was below 3% (1/37). We report 16 unrelated families with a total of 19 different *SIL1* mutations. Among these mutations are 15 previously unreported changes, including single- and multi-exon deletions. Based on data from our screening cohort and data compiled from the literature we found that *SIL1* mutations are invariably associated with the combination of a cerebellar syndrome and chronic myopathy. Cataracts were observed in all patients beyond the age of 7 years, but might be missing in infants. Six patients with *SIL1* mutations had no intellectual disability, extending the known wide range of cognitive capabilities in Marinesco-Sjögren syndrome to include normal intelligence. Modestly constant features were somatic growth retardation, skeletal abnormalities and pyramidal tract signs. Examination of mutant *SIL1* expression in cultured patient lymphoblasts suggested that *SIL1* mutations result in severely reduced *SIL1* protein levels irrespective of the type and position of mutations. Our data broaden the *SIL1* mutation spectrum and confirm that *SIL1* is the major Marinesco-Sjögren syndrome gene. *SIL1* patients usually present with the characteristic triad but cataracts might be missing in young children. As cognitive impairment is not obligatory, patients without intellectual disability but a Marinesco-Sjögren syndrome-compatible phenotype should receive *SIL1* mutation analysis. Despite allelic heterogeneity and many families with private mutations, the phenotype related to *SIL1* mutations is relatively homogenous. Based on *SIL1* expression studies we speculate that this may arise from a uniform effect of different mutations on protein expression.

Keywords: Marinesco-Sjögren syndrome; ataxia; cataract; myopathy; *SIL1* mutation

Introduction

Marinesco-Sjögren syndrome (MIM 248800) is a long-recognized autosomal recessively inherited, infantile-onset multisystem disorder that affects brain, eyes and skeletal muscles. The clinical triad of bilateral cataracts, ataxia and intellectual disability was noted in the first half of the last century (Moravcsik, 1904; Marinesco *et al.*, 1931; Sjögren, 1947) and later confirmed in a series of additional reports. Pathoanatomical and brain imaging studies revealed cerebellar atrophy as the cause of the cerebellar syndrome (Todorov, 1965; Georgy *et al.*, 1998). From histopathological and neurophysiological investigations chronic myopathy emerged as an additional feature (Chaco, 1969; Herva *et al.*, 1987) and electron microscopy revealed particular electron-dense membranous structures around degenerating myonuclei (Herva *et al.*, 1987; Sewry *et al.*, 1988). Hypergonadotropic hypogonadism, skeletal abnormalities and short stature are additional features that have been reported with variable frequency (Berg and Skre, 1976; Brogdon *et al.*, 1996). Although most patients are severely handicapped, life span in Marinesco-Sjögren syndrome is at least not drastically reduced as the oldest reported patients are in their 70s (Anttonen *et al.*, 2005). More recently, using positional cloning strategies, we and others have shown that Marinesco-Sjögren

syndrome is caused by homozygous or compound heterozygous point mutations in the *SIL1* gene on chromosome 5q31.2 (Anttonen *et al.*, 2005; Senderek *et al.*, 2005). Following the two original reports, 14 additional families with *SIL1* mutations have been described in the medical literature (Karim *et al.*, 2006; Annesi *et al.*, 2007; Anttonen *et al.*, 2008; Eriguchi *et al.*, 2008; Riazuddin *et al.*, 2009; Takahata *et al.*, 2010; Terracciano *et al.*, 2012). A subgroup of patients with Marinesco-Sjögren syndrome was found to be negative for *SIL1* point mutations, suggesting alternative mutation mechanisms or locus heterogeneity (Senderek *et al.*, 2005; Anttonen *et al.*, 2008).

SIL1, the human homolog of yeast Sil1p (suppressor of the *Aire1 Δlhs1* double mutant number 1), is an evolutionary conserved, ubiquitously expressed 461 amino-acid N-linked glycoprotein (Chung *et al.*, 2002). *SIL1* acts as a co-chaperone and nucleotide exchange factor for the HSP70 (heat-shock protein 70) ATPase BiP (immunoglobulin binding protein, also referred to as 78-kDa glucose-regulated protein GRP78) (Haas and Wabl, 1983; Munro and Pelham, 1986). BiP is a stress-inducible molecular chaperone and controls a plethora of essential processes in the endoplasmic reticulum including translocation of nascent proteins into the endoplasmic reticulum, accurate subsequent folding of the newly synthesized proteins in the endoplasmic reticulum lumen,

elimination of proteins that fail to mature properly, response to cell stress, and calcium homeostasis (Hendershot, 2004). As at least some functions of BiP require its ATPase activity, it seems plausible to assume that the nucleotide exchange factor SIL1 is involved in the regulation of endoplasmic reticulum-associated processes through control of the BiP ATPase cycle and that impaired BiP activation is the relevant pathomechanism in Marinesco-Sjögren syndrome.

The prominent cerebellar atrophy seen in patients with Marinesco-Sjögren syndrome is caused by loss of Purkinje and granule cells (Todorov, 1965; Mahloudji *et al.*, 1972; Skre and Berg, 1977). The same histopathological findings are present in the spontaneous mouse mutant *woozy*, which lacks a functional *Sil1* gene resulting in adult-onset ataxia (Zhao *et al.*, 2005). However, *woozy* mice seem to differ from humans with Marinesco-Sjögren syndrome as no symptoms like cataracts or myopathy have been described in this animal model. SIL1 is expressed in all tissues and organs in vertebrates with highest levels in secretory tissues such as liver, placenta and kidney (Chung *et al.*, 2002). It remains unknown why loss of SIL1 function in man and mice does not cause lethality and why certain tissues and cell types such as cerebellum (in mice and humans), eye and skeletal muscle (in humans) are more vulnerable to loss of SIL1 function than other tissues. As in yeast (Tyson and Stirling, 2000), the presence of the additional nucleotide exchange factor HYOU1 (also known as ORP150 and GRP170) in various organs of mammals may be able to compensate the loss of SIL1 function. This hypothesis has recently been supported by the finding that the cerebellar atrophy in the *woozy* mouse can be compensated by over-expression of HYOU1 (Zhao *et al.*, 2010).

Here, we screened a cohort of unselected patients referred for molecular genetic testing of the *SIL1* gene. We extend the phenotypic and mutation spectrum in patients with Marinesco-Sjögren syndrome and suggest inclusion criteria for *SIL1* mutation screening based on compilation of clinical data of all reported patients with *SIL1* mutations.

Materials and methods

Patients

All patients included in this study were referred to our molecular genetic diagnostic laboratory for *SIL1* mutation analysis between 2005 and 2011. The general inclusion criteria for this study required definite or probable clinical evidence of early-onset cataracts, cerebellar atrophy/ataxia and chronic myopathy ($n = 25$). We also enrolled a cohort of patients presenting with two out of the three cardinal features plus at least one of the following additional features: short stature, intellectual disability, delayed motor milestones, muscular hypotonia, hypogonadism, peripheral neuropathy, skeletal deformities (e.g. scoliosis, pes cavus) ($n = 37$). All biological materials (blood samples, DNA samples, cell lines, archived specimens of diagnostic muscle biopsies), medical and neurophysiological reports, clinical photographs, ultrasound images, and brain MRI scans were obtained under appropriate informed consent of the patients or their legal guardians. Muscle biopsies were processed as described previously (Weis and Schröder, 1988, 1989).

SIL1 gene sequence analysis

Primer sets for PCR amplification of human *SIL1* coding exons 2–10 (NM_022464.4) with 40 to 50 bp of flanking intronic sequences have been described previously (Senderek *et al.*, 2005). The resulting PCR products were subjected to fluorescence-based cycle sequencing using the BigDye[®] Terminator Cycle Sequencing Ready Reaction Kit, version 3.1 (Applied Biosystems). Samples were run and analysed on an ABI PRISM 3100 Genetic Analyzer (Applied Biosystems). Sequencing electropherograms were assessed by visual inspection in order to identify variants.

Identification of *SIL1* exon-deletion mutations

In Patient MSS87.1 we identified a seemingly homozygous mutation in exon 9 whereas we observed heterozygosity for two variants in exon 3 and intron 4. Based on these findings we assumed that Patient MSS87.1 might harbour a heterozygous intragenic deletion encompassing at least exon 9. High resolution genome wide single-nucleotide polymorphism array analysis was performed by using an Affymetrix 250K Nsp SNP array (Affymetrix), in accordance with the supplier's instructions, and copy-number data were analysed with the Affymetrix Genotyping Console 3.0.2 software. For confirmation and fine mapping of a copy number deviation, we developed quantitative real-time PCR assays for 12 fragments located in introns 7 and 9 and 3' of the *SIL1* gene (Fig. 1B). As reference locus, exon 3 of the factor VIII gene (Wilke *et al.*, 2000) was used. Quantitative real-time PCR was carried out on an ABI PRISM 7000 sequence detection system (Applied Biosystems) using the quantitative real-time PCR core kit for SYBR Green I according to the manufacturer's protocol (Eurogentec). Data evaluation was performed using the ABI PRISM 7000 sequence detection software as described previously (Wilke *et al.*, 2000) and the ratios of test and reference fragments were calculated to determine copy numbers of the test fragments. Primers from the fragments found to be situated just outside the deletion (i.e. fragments yielding results in favour of two copies) were used in an attempt to amplify the breakpoint region by long-range PCR.

PCR amplification of *SIL1* exon 5 consistently failed in the DNA sample of the index patient of Family MSS150.1 whereas amplification of exons 4 and 6 was normal. To obtain further evidence for a presumed intragenic deletion removing exon 5, total RNA was isolated from a fresh blood sample of the index patient, reverse transcribed and used as template for PCR with primers in *SIL1* exons 1 and 10 (Fig. 1C). Sequencing of the PCR product was performed using ABI Prism BigDye[®] technology as described above. At the genomic level, the extent of the presumed deletion was defined using amplification of several short 100–200 bp genomic fragments placed every 2–3 kb within the 25 kb genomic region encompassing intron 4, exon 5 and intron 5. Primers from fragments found to lie just outside the deletion (i.e. these fragments yielded amplification in patient's DNA while fragments situated in the genomic region flanked by these markers gave no products) were combined to amplify a junction fragment characteristic for the deletion (Fig. 1D). The junction fragment was subjected to cycle sequencing in order to identify the precise positions of the deletion breakpoints.

Cell culture and western blotting

Epstein-Barr virus-immortalized B lymphoblast cell lines from control subjects and patients with Marinesco-Sjögren syndrome were established

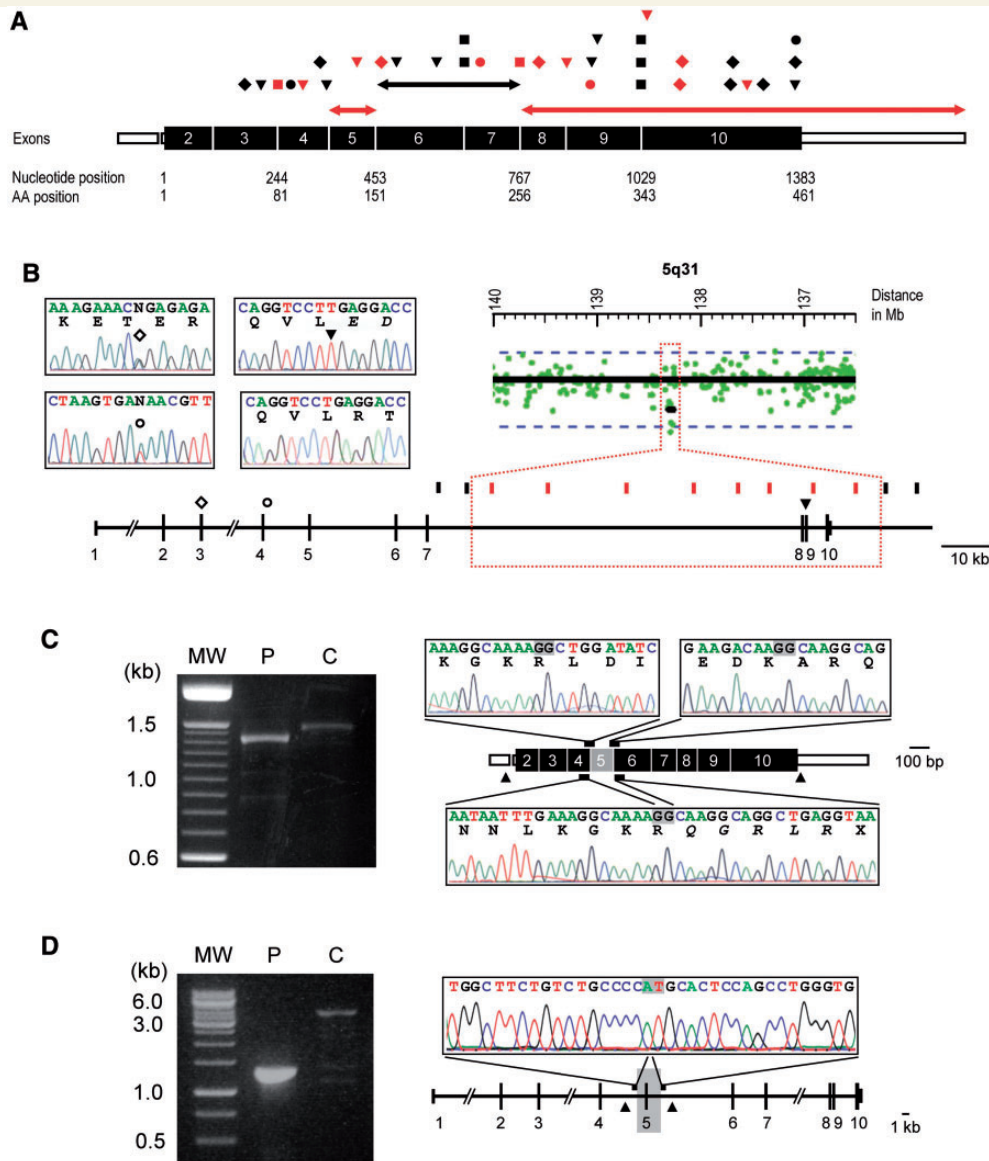


Figure 1 *SIL1* mutations. (A) Graphical overview of mutations found in this and other studies. Different mutation types are marked with different symbols. Circles = missense mutations and small in-frame indels; rhombi = nonsense mutations; triangles = frameshift mutations; squares = splice site mutations; two-sided arrows = exon-deletion mutations. Previously unreported sequence variations identified in this study are coloured in red. Exon, nucleotide and amino acid numbering is according to NM_022464.4 and NP_071909.1. Introns are not drawn to scale. AA = amino acid. (B) Heterozygous multi-exon deletion in Patient MSS87.1. Sequencing electropherograms show heterozygous variants in exon 3 (rs3088052, open rhombus) and intron 4 (c.353 + 38T > A, open circle) as well as a seemingly homozygous frameshift mutation c.947dupT, p.R317fs in exon 9 (filled triangle), the electropherogram below represents the wild-type sequence). A high-density genome-wide single nucleotide polymorphism array (upper left) and copy number analysis of fragments located in the potential deletion region by quantitative real-time PCR (vertical bars above the schematic representation of the *SIL1* gene, red: one copy, black: two copies) were suggestive of a partial, ~68–77 kb deletion involving exons 8–10 (boxed with dotted red lines). Long-range PCR with primers from the fragments found to be situated just outside the deletion failed to amplify a deletion specific junction fragment leaving the possibility of a more complex genomic rearrangement although routine-karyotyping had previously shown two normal chromosomes 5. (C and D) Homozygous exon 5 deletion in Patient MSS150.1. (C) Reverse transcription PCR using patient's messenger RNA (P) yielded a shorter 1370-bp fragment (C: control messenger RNA, 1470 bp). Positions of primers are indicated by arrowheads underneath the schematic representation of the *SIL1* messenger RNA. Sequencing electropherograms representing the normal exon 4/exon 5 and normal exon 5/exon 6 junctions are shown above the schematic representation of the *SIL1* messenger RNA; the exon 4/exon 6 junction resulting from the genomic deletion is shown below. Removal of the 100-bp exon 5 from the mature messenger RNA is predicted to result in frameshift and premature stop of translation (asterisk). (D) Sequencing of a PCR-amplified deletion-specific junction fragment at the genomic level. Primers placed in intron 4 and intron 5 of the *SIL1* gene yielded a ~2.5 kb shorter product when using patient's (P) DNA (C: control DNA, 4029 bp). Positions of primers are indicated by arrowheads underneath the schematic representation of the *SIL1* gene genomic region (not drawn to scale). The borders of the deletion which encompasses 2660 bp including exon 5 were determined by DNA sequencing with internal primers. The extent of the deletion is indicated as a grey box.

according to standard protocols (Tohda *et al.*, 1978). The immortalized lymphoblasts were cultured in RPMI-1640 growth medium, harvested by centrifugation (800 rpm, 7 min), washed twice in cold PBS and pelleted by centrifugation (14 000 rpm, 5 min, 4°C). Cell pellets were homogenized in lysis buffer (10 mM Tris-HCl, 5 mM EDTA, 150 mM NaCl, 1% Triton™ X-100) containing protease and phosphatase inhibitors. Post-nuclear supernatants were boiled in sample buffer (80 mM Tris pH 6.8, 10% glycerol, 2% SDS, 0.002% bromophenol blue), resolved by SDS-PAGE and electroblotted onto polyvinylidene fluoride membranes (Hybond-C; GE Healthcare). Immunoblots were developed by incubation with appropriate antibodies followed by horseradish peroxidase-phosphatase chemiluminescence detection (ECL; GE Healthcare). The following antibodies were used: mouse monoclonal anti-SIL1 clone 1F9 (Origene Technologies; dilution 1:1000), mouse monoclonal anti-GAPDH (Genetex; dilution 1:1000), goat anti-rabbit immunoglobulin G antibody conjugated to horseradish peroxidase (Invitrogen; dilution 1:5000), goat anti-mouse immunoglobulin G conjugated to horseradish peroxidase (Invitrogen; dilution 1:5000).

Results

Mutation screening of the *SIL1* gene in a diagnostic sample of 62 unrelated, previously unreported index patients with Marinesco-Sjögren syndrome or Marinesco-Sjögren syndrome-like conditions revealed pathogenic sequence variants in 16 families of diverse ethnic backgrounds, representing roughly 25% of the total cohort. The mutation detection rate reached 60% (15/25) in the cohort of patients presenting with the clinical triad of cerebellar atrophy, myopathy and cataracts whereas the mutation detection rate was <3% (1/37) among Marinesco-Sjögren syndrome-like cases (two of the cardinal features and at least one of the following symptoms: short stature, intellectual disability, delayed motor milestones, hypotonia, hypogonadism, peripheral neuropathy, skeletal deformities).

We observed a total of 19 different *SIL1* mutations consisting of a missense mutation, a two-amino acid in-frame deletion, seven frameshift mutations, four nonsense mutations, four nucleotide changes affecting splice sites and two genomic deletions (Fig. 1 and Table 1). Among these mutations, 15 had not been reported previously. None of these so far unrecognized changes was present in databases containing information on the 'normal' variability of the human genome (dbSNP version 135, www.1000genomes.org/; 1000 Genomes database, www.ncbi.nlm.nih.gov/projects/SNP/; Exome Variant Server, evs.gs.washington.edu/EVS/). In addition, analysis of DNA samples obtained from healthy control individuals, adjusted to the type of mutation (i.e. at least 100 for each truncating and at least 400 for each missense mutation), did not yield any of the identified genotypes. All patients were identified with bi-allelic mutations, either in the homozygous or compound heterozygous state. When DNA from family members was available, we observed that the disease phenotype co-segregated with recessive inheritance of the *SIL1* mutations. The parents carried mutations in the heterozygous state, and unaffected siblings carried either one heterozygous mutation or were homozygous for the wild-type alleles.

Detailed clinical, electrophysiological and muscle biopsy findings of 23 patients from the 16 families carrying pathogenic *SIL1* mutations are provided in Supplementary Table 1. All patients came to medical

attention with symptoms suggestive of Marinesco-Sjögren syndrome within the first 5 years of life. Initial presenting symptoms were nonetheless variable: some patients presented very soon after birth with severe hypotonia, whereas most showed delay in motor milestones or truncal ataxia when starting to sit or stand, after a normal neonatal period. The mean age at onset of cataracts was 3.7 years (± 1.5 years). Congenital cataracts were only noted in one patient and the latest manifestation of cataracts was reported at the age of 7 years. In line with this observation, one girl did not show any lens opacities at the age of 4 years. Apart from this exception, all patients invariably presented with a cerebellar syndrome, symptoms and signs of a myopathy and bilateral cataracts. Modestly constant features were skeletal deformities, somatic growth retardation and pyramidal tract signs. Mental capacities of patients with *SIL1* mutations were highly variable, ranging from normal ($n = 6$) over mild ($n = 7$) to moderate ($n = 8$) and severe intellectual disability ($n = 2$). Other clinical features were only occasionally recorded (e.g. epilepsy or microcephaly) or could only be reasonably assessed in a too small subgroup of patients to give meaningful figures (e.g. hypogonadism in postpubertal patients). Although motor development was often markedly delayed, patients generally became mobile with a walker or other orthopaedic devices (canes, crutches, braces). Marked atrophy of the cerebellum was observed in all patients who received brain MRI (Fig. 2B–D). Serum creatine kinase (CK) levels were usually only slightly or moderately elevated (377 ± 159 U/l). Through a review of the medical literature we recorded 65 additional patients with Marinesco-Sjögren syndrome with confirmed *SIL1* mutations (30 families). We combined these data with information from our patient cohort to determine the relative frequency of signs and symptoms in *SIL1*-associated Marinesco-Sjögren syndrome (Supplementary Table 2 and Fig. 2A).

We reassessed muscle biopsy specimens that had been taken for diagnostic purposes from four patients with identified *SIL1* mutations (MSS33.1, MSS87.1, MSS91.1, and MSS94.1). Histologically we observed different degrees of degeneration of skeletal muscle fibres (Fig. 3A): sarcoplasmic vacuoles, often associated with myonuclei, greater-than-normal variability in fibre size, rounded atrophic fibres, myofibre hypertrophy and splitting, increased numbers of internal nuclei, endomysial fibrosis and proliferation of fat tissue. At the ultrastructural level (Fig. 3B–D), autophagic vacuoles, which were often associated with degenerating myonuclei, were encountered frequently. Several degenerating myonuclei were surrounded by an electron-dense, membrane-like structure. This feature was constantly observed in all four muscle biopsies that were accessible to us. Muscle biopsy findings of 10 additional patients were available from medical records and were indicative of a chronic myopathic process. Five biopsy samples had also been examined by electron microscopy; however, no details concerning possible nuclear abnormalities were mentioned in the reports.

By immunoblotting, we found that SIL1 levels in lymphoblast lines of five patients with different *SIL1* mutations were substantially reduced compared with the levels in control subjects (Fig. 4). Importantly, reduced amounts of SIL1 were also seen in patients with seemingly 'milder' mutations [small in-frame deletion (MSS24.1), missense mutation (MSS32.1) and frameshift mutation in the last exon which is expected to escape nonsense-mediated messenger RNA decay (MSS64.1)].

Table 1 *SIL1* mutations in patients with Marinesco-Sjögren syndrome identified in this study and earlier reports

Location	Nucleotide change	Effect on coding sequence	Ethnic origin	References
Exon 3	c.178G>T	p.E60X	Vietnam	Senderek <i>et al.</i> , 2005
Exon 3	c.212dupA	p.H71fs	France	Anttonen <i>et al.</i> , 2005
Intron 3	c.244 + 1G>A	splice error predicted	Turkey	This study
Exon 4	c.274C>T	p.R92W	Pakistan	Riazuddin <i>et al.</i> , 2009
Exon 4	c.302_303delAG	p.E101fs	Pakistan	This study
Exon 4	c.331C>T	p.R111X	Iran, Turkey, Italy	Senderek <i>et al.</i> , 2005 Anttonen <i>et al.</i> , 2005 Annesi <i>et al.</i> , 2007 Terracciano <i>et al.</i> , 2012
Exon 4	c.347delG	p.G116fs	Vietnam	Senderek <i>et al.</i> , 2005
Exon 5	chr5:g.138376244_138378903del	p.L119fs	India	This study
Exon 5	c.424delG	p.A142fs	Germany	This study
Exons 6, 7	chr5:g.138311133_138369401delinsTGCA	p.A152fs	Japan	Takahata <i>et al.</i> , 2010
Exon 6	c.460C>T	p.Q154X	France	This study
Exon 6	c.506_509dupAAGA	p.D170fs	Finland, Sweden, Norway	Anttonen <i>et al.</i> , 2005
Exon 6	c.603_607delGAAGA	p.E201fs	Japan	Takahata <i>et al.</i> , 2010
Intron 6	c.645 + 1G>A	p.A152_Q215del	Turkey, Argentina	Senderek <i>et al.</i> , 2005 This study
Intron 6	c.645 + 2T>C	p.A152_Q215del	Sweden	Anttonen <i>et al.</i> , 2005
Exon 7	c.691_696delGTGATC	p.V231_I232del	Turkey	This study
Intron 7	c.768-1G>A	p.S256fs	Italy	This study
Exons 8, 9, 10	chr5:g.(138271912_138277581) _(138345106_138349134)del	p.S256_R461del	Russia	This study
Exon 8	c.811C>T	p.Q271X	Turkey	This study
Exon 9	c.866dupT	p.L290fs	France	This study
Exon 9	c.934G>A	p.G312R	USA	This study
Exon 9	c.936dupG	p.L313fs	Japan, Argentina	Eriguchi <i>et al.</i> , 2008 Anttonen <i>et al.</i> , 2008 This study
Exon 9	c.947dupT	p.R317fs	Germany, Russia	Senderek <i>et al.</i> , 2005 This study
Intron 9	c.1029 + 1G>A	p.V289_K343del	Bosnia	Senderek <i>et al.</i> , 2005
Intron 9	c.1030-9G>A	p.F345fs	Norway, USA, Pakistan	Anttonen <i>et al.</i> , 2008 This study
Intron 9	c.1030-18G>A	p.M344fs	Germany	Senderek <i>et al.</i> , 2005
Exon 10	c.1035delC	p.F345fs	Germany	This study
Exon 10	c.1126C>T	p.Q376X	Pakistan	This study
Exon 10	c.1137C>A	p.C379X	Iraq	This study
Exon 10	c.1240C>T	p.Q414X	Pakistan	Riazuddin <i>et al.</i> , 2009
Exon 10	c.1249C>T	p.Q417X	Mali	Senderek <i>et al.</i> , 2005
Exon 10	c.1276_1282delCAGGCTG	p.Q426fs	Germany	This study
Exon 10	c.1312C>T	p.Q438X	Egypt	Karim <i>et al.</i> , 2006
Exon 10	c.1367delT	p.L456fs	Russia	Senderek <i>et al.</i> , 2005
Exon 10	c.1367T>A	p.L456X	Turkey	Anttonen <i>et al.</i> , 2008
Exon 10	c.1370T>C	p.L457P	Japan	Anttonen <i>et al.</i> , 2008

Exon, nucleotide and amino acid numbering is according to NM_022464.4 and NP_071909.1. Genomic coordinates are based on GRCh37/hg19.

Discussion

In this study we report the results of *SIL1* mutation screening in patients who were referred to our laboratory for molecular genetic testing of Marinesco-Sjögren syndrome during the past 5 years. Our study confirms the previous findings of mutations in *SIL1* being the major cause of Marinesco-Sjögren syndrome. Our data extend the spectrum of Marinesco-Sjögren syndrome-causing *SIL1* mutations, increasing the number of different mutations to 36 and bringing the total number of published molecular-genetically

confirmed families to 46 (88 patients). Based on these data we describe the relative frequency of signs and symptoms of patients with Marinesco-Sjögren syndrome with identified *SIL1* mutations. This information may help to decide which patients should undergo *SIL1* mutation analysis.

We confirm that Marinesco-Sjögren syndrome caused by *SIL1* mutations is a panethnic condition. Some *SIL1* mutations have been found as recurrent events in more than one family and four mutations have been found repeatedly ($\geq 3 \times$) in independent families (p.R111X, p.D170fs, p.R317fs, p.F345fs, Table 1).

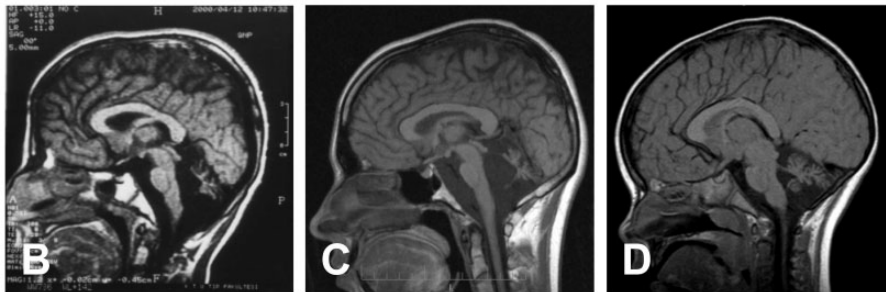
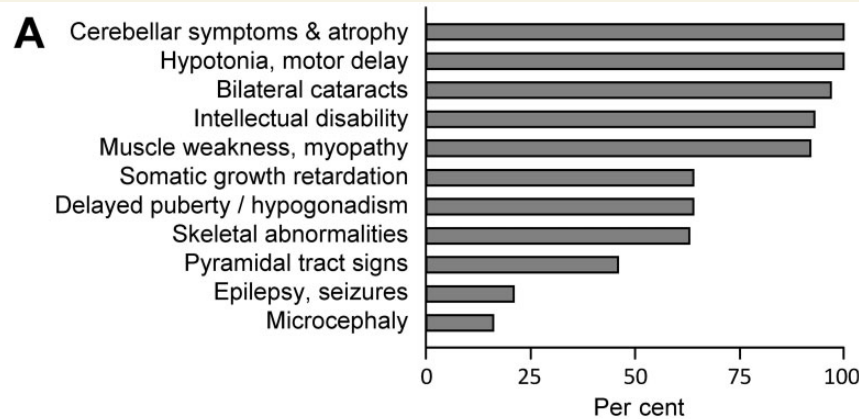


Figure 2 Clinical presentation of patients with Marinesco-Sjögren syndrome with identified *SIL1* mutations. (A) Relative frequency of signs and symptoms based on data compiled from our patient cohort and reports from the literature (Anttonen *et al.*, 2005; Senderek *et al.*, 2005; Karim *et al.*, 2006; Annesi *et al.*, 2007; Anttonen *et al.*, 2008; Eriguchi *et al.*, 2008; Riazuddin *et al.*, 2009; Takahata *et al.*, 2010; Terracciano *et al.*, 2012). For details see Supplementary Tables 1 and 2. (B–D) Sagittal MRI scans of three patients with Marinesco-Sjögren syndrome showing marked cerebellar atrophy. (B) Patient MSS25.2 at age 14 years, T₁-weighted image; (C) Patient MSS33.1 at age 24 years, T₁-weighted image; (D) Patient MSS87.1 at age 3 years, T₁-weighted image.

However, most mutations are private mutations identified in single families only making diagnostic recommendations for selected screening of exons or testing of selected mutations arguable. Most pathogenic variants identified in this study and reported earlier are micromutations affecting one or a few nucleotides. Moreover, we and others (Takahata *et al.*, 2010) found that the *SIL1* mutation spectrum also includes deletions of several kb of DNA. Although it is conceivable that some patients without an identified *SIL1* mutation are compound heterozygous for non-overlapping genomic deletions in the huge *SIL1* gene (spanning ~0.25 Mb of genomic DNA), data from whole-genome single nucleotide polymorphism genotyping and copy number variation analysis available for 29 out of the 46 *SIL1* mutation-negative patients (A. Roos and S. Spengler, unpublished data) showed no genetic imbalances of the *SIL1* gene that is covered by 115 markers on the microarrays used (Affymetrix GeneChip Genome-Wide Human SNP 6.0-Array, Supplementary Fig. 1). Nevertheless, it is probably warranted to extend future *SIL1* mutation screening to investigate the presence of pathogenic copy number aberrations. In addition to mutations missed by commonly applied diagnostic strategies there is evidence for locus heterogeneity as well. We excluded linkage or homozygosity to the *SIL1* region on chromosome 5 in four families with a typical Marinesco-Sjögren syndrome phenotype confirming that at least one additional locus does exist (Families MSS96, MSS136, MSS144, MSS174). Others have

explored functional candidate genes for mutations in unclarified Marinesco-Sjögren syndrome cases without success (Anttonen *et al.*, 2008).

Although Marinesco-Sjögren syndrome is caused by a wide spectrum of *SIL1* mutations, patients present with a relatively homogeneous phenotype and show almost invariably the hallmark clinical features of cerebellar atrophy and ataxia, cataracts, intellectual disability and myopathy (Fig. 2). These somewhat contradictory observations might be reconciled by the notion that all *SIL1* mutations are expected to eventually lead to loss of the protein or its critical functional domains. This has been predicted or experimentally confirmed for most nonsense and frameshift mutations (Senderek *et al.*, 2005) and for mutations altering the very C-terminus of the protein (Howes *et al.*, 2012). In the present study we have shown that a *SIL1* missense mutation (p.G312R), a two amino acid in-frame deletion (p.V231_I232del) and a frameshift mutation in the last exon, which is predicted to escape nonsense-mediated messenger RNA decay (p.Q426fs), also result in a prominent reduction of SIL1 protein levels in cultured lymphoblasts (Fig. 4). Although we cannot conclude from these data that reduced protein levels are a general consequence of seemingly 'milder' *SIL1* mutations, such a mechanism might exist for at least a subset of mutations, and for some it has been experimentally shown that mutant proteins are particularly

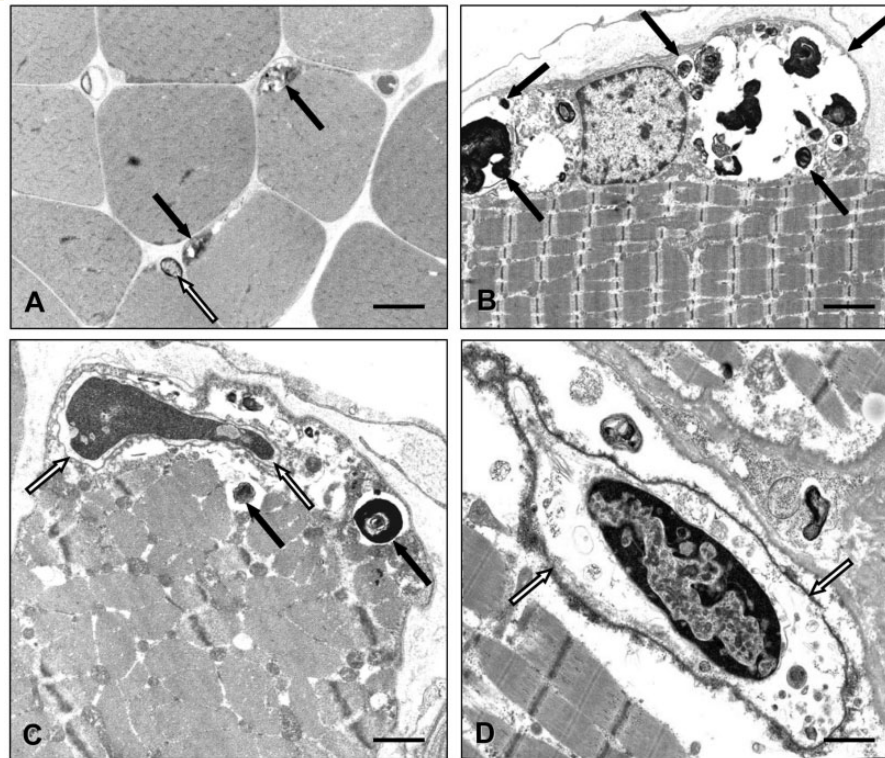


Figure 3 Histopathological and electron microscopic findings in skeletal muscle biopsies of patients with Marinesco-Sjögren syndrome. (A) Patient MSS33.1. Black arrows: abnormal nuclei and autophagic material. White arrow: normal myonucleus. Semi-thin section of glutaraldehyde-fixed, epon-embedded tissue; toluidine blue. Scale bar = 20 μm . (B) Patient MSS87.1. Arrows: autophagic vacuoles in the perinuclear sarcoplasm. Ultra-thin section of glutaraldehyde-fixed, epon-embedded tissue; electron microscopy. Scale bar = 3 μm . (C) Patient MSS87.1. Black arrows: autophagic vacuoles in the perinuclear sarcoplasm of an atrophic muscle fibre. White arrows: perinuclear osmiophilic membrane-like structure characteristic for Marinesco-Sjögren syndrome. The myonucleus shows degenerative condensation of chromatin. Electron microscopy. Scale bar = 2.5 μm . (D) Patient MSS33.1. Arrows: degenerating myonucleus ensheathed by a prominent osmiophilic membrane-like structure. Electron microscopy. Scale bar = 1.5 μm .

unstable and either form large aggregates in the endoplasmic reticulum or are rapidly degraded through the proteasome (Howes *et al.*, 2012).

Our data confirm that the clinical triad of cataracts, cerebellar atrophy and myopathy strongly suggests the presence of *SIL1* mutations (detection rate 60%) whereas patients presenting with variant phenotypes are unlikely to have *SIL1* mutations (detection rate 2.7%). The only mutation-positive case in the latter cohort was a girl who had not developed cataracts until the age of 4 years (Patient MSS24.1). Two additional patients without cataracts (at age 1 and 4 years, respectively) have been reported (Senderek *et al.*, 2005; Terracciano *et al.*, 2012). As the latest reported onset of cataracts was in a 7-year-old girl in our cohort (Patient MSS142.1), these patients are likely to develop cataracts within the next few years. It has been noted previously that cataracts may develop unusually fast within a few weeks in patients with Marinesco-Sjögren syndrome (Ishikawa *et al.*, 1993). Therefore it might be appropriate to include infants and preschool age children with cerebellar atrophy and myopathy without cataracts in *SIL1* mutation screening while the full-blown phenotype including cataracts should be expected after the age of 10 years. Historical descriptions of patients with Marinesco-Sjögren

syndrome stressed the presence of profound intellectual disability in most cases (Müller, 1962; Hayabara *et al.*, 1975). More recent reports showed a large spectrum of mental impairment in Marinesco-Sjögren syndrome with most patients exhibiting only mild cognitive impairment and only few cases with severe intellectual deficits. In our cohort of patients with *SIL1* mutations we identified six cases with normal intellectual capacities but an otherwise typical Marinesco-Sjögren syndrome phenotype (Fig. 5). Patients without intellectual disability should be considered for *SIL1* mutation analysis if their clinical presentation was compatible with the diagnosis of Marinesco-Sjögren syndrome.

The differential diagnosis of Marinesco-Sjögren syndrome includes several conditions featuring combinations of brain, skeletal muscle and eye abnormalities. Congenital cataracts, facial dysmorphism, and neuropathy syndrome shares with Marinesco-Sjögren syndrome the features of cataracts and muscle weakness or hypotonia. The presence of cerebellar atrophy in Marinesco-Sjögren syndrome and demyelinating neuropathy in congenital cataracts, facial dysmorphism, and neuropathy syndrome distinguishes the two syndromes (Lagier-Tourenne *et al.*, 2002). Congenital cataracts, facial dysmorphism, and neuropathy syndrome is caused by a founder mutation in the *CTDP1* gene

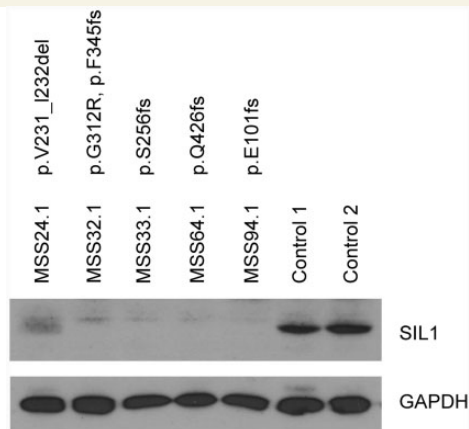


Figure 4 *SIL1* mutations result in substantially decreased *SIL1* protein levels. Immunoblot of *SIL1* in immortalized lymphoblasts of patients with Marinesco-Sjögren syndrome. Cell lysates of Patients MSS24, MSS32, MSS33, MSS64 and MSS94 and two healthy control individuals were immunoblotted with an anti-*SIL1* antibody (*top*) and an anti-GAPDH antibody (as loading control, *bottom*). *SIL1* levels in patients' lymphoblasts were severely reduced compared to the levels in control subjects. Note that seemingly 'milder' mutations [small in-frame deletion (MSS24.1), missense mutation (MSS32.1) and frameshift mutation in the last exon (MSS64.1)] have similar effects as truncating mutations that are expected to lead to nonsense-mediated messenger RNA decay (MSS33.1 and MSS94.1).

(Varon *et al.*, 2003) that seems to be restricted to the Gypsy population. In fact, two patients from our cohort of Marinesco-Sjögren syndrome-like cases, both of Gypsy origin and presenting with congenital cataracts and a history of hypotonia, muscle weakness and elevated creatine kinase levels initially suggesting a myopathic process were found to carry the *CTDP1* founder mutation. Careful clinical and neurophysiological re-evaluation revealed a demyelinating neuropathy as the cause of the neuromuscular features (Patients MSS21.1 and MSS73.1, Supplementary Table 3). Cerebrotendinous xanthomatosis is an inherited disorder associated with the deposition of cholestanol in the brain and other tissues and is characterized by progressive cerebellar ataxia, cataracts, and tendinous or tuberous xanthomas (Van Bogaert *et al.*, 1937). The diagnosis can be made by elevated serum cholestanol levels and identification of mutations in the *CYP27A1* gene (Cali *et al.*, 1991). Importantly, cerebrotendinous xanthomatosis is a treatable condition warranting proper diagnostic measures to be taken (Berginer *et al.*, 1984). One patient with juvenile cataracts and neurological problems starting during adolescence included in our series (Patient MSS48.1, Supplementary Table 3) was found to have cerebrotendinous xanthomatosis. Other differential diagnoses include ataxia-microcephaly-cataract syndrome (Ziv *et al.*, 1992), cataract-ataxia-deafness-retardation syndrome (Begeer *et al.*, 1991) and *VLDLR*-associated cerebellar hypoplasia (Schurig *et al.*, 1981; Boycott *et al.*, 2005). Finally, Marinesco-Sjögren syndrome shares clinical features with mitochondrial disorders (Schapira, 2006) and disorders of defective N- and O-glycosylation of proteins (Eklund and Freeze, 2006;

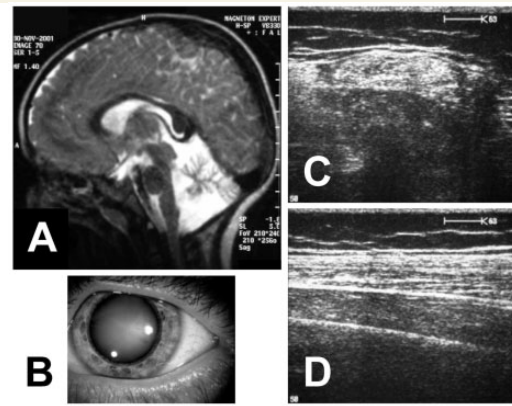


Figure 5 Patient MSS64.1 without intellectual disability but an otherwise characteristic Marinesco-Sjögren syndrome phenotype. (A) Brain MRI scan at age 20 months shows profound atrophy of the cerebellum (T₂-weighted image). (B) Cataract of the right eye which developed within a few weeks at age 3.5 years. (C and D) Sonography of the M. quadriceps at the age of 6.75 years shows an increase in echogenicity, especially in the area of the M. rectus femoris with poorly identifiable structures of fascia and lack of echogenicity of the bone.

Muntoni *et al.*, 2011). One of the *SIL1* mutation-negative patients in our series (Patient MSS53.1, Supplementary Table 3) was diagnosed with Sengers syndrome, a form of mitochondrial DNA depletion disorder caused by an *AGK* gene mutation (Calvo *et al.*, 2012; Mayr *et al.*, 2012).

To our knowledge, there are no comprehensive screening studies that have explored a potential role of *SIL1* mutations in cohorts of patients with non-syndromic, isolated myopathy, cataracts or ataxia. However, we assume that *SIL1* has only a minor relevance in the screening of these patients. Data obtained using whole-exome sequencing and next generation sequencing ataxia panels (including all known genes for isolated or syndromic ataxias) did not reveal clearly pathogenic *SIL1* alleles in a cohort of >90 patients with early-onset ataxia that had already been screened negative for all common early-onset ataxia genes (i.e. *FXN*, *AOA2*, *AOA1*, *POLG*), thus highly enriched for mutations in rarer early onset ataxia genes (M. Synofzik and P. Bauer, unpublished data).

Muscle biopsies obtained from patients with Marinesco-Sjögren syndrome show various non-specific signs indicating degeneration of skeletal muscle fibres. At the ultrastructural level, degenerating myonuclei are occasionally surrounded by an electron-dense, membrane-like structure (Herva *et al.*, 1987; Sewry *et al.*, 1988). We have confirmed this finding in all muscle biopsies of patients with Marinesco-Sjögren syndrome that were available for electron microscopy in this study ($n=4$; MSS33.1, MSS87.1, MSS91.1 and MSS94.1) and in our earlier report ($n=6$) (Senderek *et al.*, 2005) suggesting that this finding is a characteristic feature related to *SIL1* pathology. In general, muscle biopsies are considered invasive procedures that are best avoided if a diagnosis can be established using other methods. Although with the availability of *SIL1* sequencing there is no longer a diagnostic need

for muscle biopsies in patients with Marinesco-Sjögren syndrome with typical symptoms, this procedure still may be important in the diagnosis of Marinesco-Sjögren syndrome, especially in less clear-cut cases. First of all a muscle biopsy can be helpful in differentiating myopathy from other causes of hypotonia and weakness. Secondly, the full Marinesco-Sjögren syndrome phenotype might not be seen in very young children as cataracts tend to develop later making the differentiation from other causes of a cerebellar syndrome and hypotonia more difficult. In addition, as parts of the EMG procedure (to establish a myopathy) are uncomfortable and not well tolerated by young children, results might be inconclusive. In this scenario, electron microscopy of a muscle biopsy unveiling vacuolar myopathy and the characteristic perinuclear membrane-like structures can help to consider Marinesco-Sjögren syndrome as a differential diagnosis and can direct to *SIL1* mutation analysis (Terracciano *et al.*, 2012).

The current study contributes to our understanding of the clinical and genetic basis of Marinesco-Sjögren syndrome. A molecular diagnosis was obtained in ~60% of patients from a screening cohort of 25 unrelated index patients with a full-blown Marinesco-Sjögren syndrome phenotype leaving a considerable proportion of patients without genetic diagnosis to date. This further underscores the fact that other still unknown mutations must exist in known or unknown disease associated genes. As a co-chaperone for BiP, *SIL1* is involved in protein synthesis and quality control in the endoplasmic reticulum. Thus, secretory pathway proteins not properly processed or not reaching their site of action in *SIL1* deficient cells will represent plausible functional candidates. No such factors have been identified so far, but appropriate tools for proteomic analysis of cell compartments and cell surface proteins are now at hand. Combining such data with data obtained by high-throughput DNA sequencing projects in non-*SIL1* Marinesco-Sjögren syndrome families will likely disclose the missing Marinesco-Sjögren syndrome gene(s) within the next few years and may also hold promise to identify potential therapeutic targets.

Acknowledgements

We wish to thank the patients and their families for participating in this study. The skilful technical assistance of Ms Irmgard Diepolder is gratefully acknowledged.

Funding

This work has been supported by grants from the Maximilian-May-Stiftung, the Gebert-Rüf-Stiftung (to J.S., grant no GRS-046/09) and the Else-Kröner-Fresenius-Stiftung (to A.R., grant no A59-09).

Supplementary material

Supplementary material is available at *Brain* online.

References

- Annesi G, Aguglia U, Tarantino P, Annesi F, De Marco EV, Civitelli D, et al. *SIL1* and *SARA2* mutations in Marinesco-Sjögren and chylomicron retention diseases. *Clin Genet* 2007; 71: 288–9.
- Anttonen AK, Mahjneh I, Hämäläinen RH, Lagier-Tourenne C, Kopra O, Waris L, et al. The gene disrupted in Marinesco-Sjögren syndrome encodes *SIL1*, an HSPA5 cochaperone. *Nat Genet* 2005; 37: 1309–11.
- Anttonen AK, Siintola E, Tranebjaerg L, Iwata NK, Bijlsma EK, Meguro H, et al. Novel *SIL1* mutations and exclusion of functional candidate genes in Marinesco-Sjögren syndrome. *Eur J Hum Genet* 2008; 16: 961–9.
- Begeer JH, Scholte FA, van Essen AJ. Two sisters with mental retardation, cataract, ataxia, progressive hearing loss, and polyneuropathy. *J Med Genet* 1991; 28: 884–5.
- Berg K, Skre H. Possible linkage between the Marinesco-Sjögren syndrome and hypergonadotropic hypogonadism. *Cytogenet Cell Genet* 1976; 16: 271–4.
- Berginer VM, Salen G, Shefer S. Long-term treatment of cerebrotendinous xanthomatosis with chenodeoxycholic acid. *N Eng J Med* 1984; 311: 1649–52.
- Boycott KM, Flavell S, Bureau A, Glass HC, Fujiwara TM, Wirrell E, et al. Homozygous deletion of the very low density lipoprotein receptor gene causes autosomal recessive cerebellar hypoplasia with cerebral gyral simplification. *Am J Hum Genet* 2005; 77: 477–83.
- Brogdon BG, Snow RD, Williams JP. Skeletal findings in Marinesco-Sjögren syndrome. *Skeletal Radiol* 1996; 25: 461–5.
- Cali JJ, Hsieh CL, Francke U, Russell DW. Mutations in the bile acid biosynthetic enzyme sterol 27-hydroxylase underlie cerebrotendinous xanthomatosis. *J Biol Chem* 1991; 266: 7779–83.
- Calvo SE, Compton AG, Hershman SG, Lim SC, Lieber DS, Tucker EJ, et al. Molecular diagnosis of infantile mitochondrial disease with targeted next-generation sequencing. *Sci Transl Med* 2012; 4: 118ra10.
- Chaco J. Marinesco-Sjögren syndrome with myopathy. *Confin Neurol* 1969; 31: 349–51.
- Chung KT, Shen Y, Hendershot LM. BAP, a mammalian BiP-associated protein, is a nucleotide exchange factor that regulates the ATPase activity of BiP. *J Biol Chem* 2002; 277: 47557–63.
- Eklund EA, Freeze HH. The congenital disorders of glycosylation: a multifaceted group of syndromes. *NeuroRx* 2006; 3: 254–63.
- Eriguchi M, Mizuta H, Kurohara K, Fujitake J, Kuroda Y. Identification of a new homozygous frameshift insertion mutation in the *SIL1* gene in 3 Japanese patients with Marinesco-Sjögren syndrome. *J Neurol Sci* 2008; 270: 197–200.
- Georgy BA, Snow RD, Brogdon BG, Wertelecki W. Neuroradiologic findings in Marinesco-Sjögren syndrome. *AJNR Am J Neuroradiol* 1998; 19: 281–3.
- Haas IG, Wabl M. Immunoglobulin heavy chain binding protein. *Nature* 1983; 306: 387–9.
- Hayabara T, Yabuki S, Ikeda H, Otsuki S. A case of oligophrenic cerebello-lental degeneration associated with vascular hypertension and gynecomastia. *Rinsho Shinkeigaku* 1975; 15: 110–5.
- Hendershot LM. The ER function BiP is a master regulator of ER function. *Mt Sinai J Med* 2004; 71: 289–97.
- Herva R, von Wendt L, von Wendt G, Saukkonen AL, Leisti J, Dubowitz V. A syndrome with juvenile cataract, cerebellar atrophy, mental retardation and myopathy. *Neuropediatrics* 1987; 18: 164–9.
- Howes J, Shimizu Y, Feige MJ, Hendershot LM. C-terminal mutations destabilize *SIL1/BAP* and can cause Marinesco-Sjögren syndrome. *J Biol Chem* 2012; 287: 8552–60.
- Ishikawa T, Kitoh H, Awaya A, Nonaka I. Rapid cataract formation in Marinesco-Sjögren syndrome. *Pediatr Neurol* 1993; 9: 407–8.
- Karim MA, Parsian AJ, Cleves MA, Bracey J, Elsayed MS, Elsobky E, et al. A novel mutation in *BAP/SIL1* gene causes Marinesco-Sjögren syndrome in an extended pedigree. *Clin Genet* 2006; 70: 420–3.
- Lagier-Tourenne C, Chaigne D, Gong J, Flori J, Mohr M, Ruh D, et al. Linkage to 18qter differentiates two clinically overlapping

- syndromes: congenital cataracts-facial dysmorphism-neuropathy (CCFDN) syndrome and Marinesco-Sjögren syndrome. *J Med Genet* 2002; 39: 838–43.
- Mahloudji M, Amirhakimi GH, Haghighi P, Khodadoust AA. Marinesco-Sjögren syndrome. Report of an autopsy. *Brain* 1972; 95: 675–80.
- Marinesco G, Draganescu S, Vasiliu D. Nouvelle maladie familiale caractérisée par une cataracte congénitale et un arrêt du développement somato-neuro-psychique. *L'encéphale* 1931; 26: 97–109.
- Mayr JA, Haack TB, Graf E, Zimmermann FA, Wieland T, Haberberger B, et al. Lack of the mitochondrial protein acylglycerol kinase causes Sengers syndrome. *Am J Hum Genet* 2012; 90: 314–20.
- Moravcsik EE. Friedreich'sche hereditäre Ataxie. *Orvosi Hetilap* 1904; 25.
- Müller K. Das Marinesco-Sjögren-Syndrom: spinocerebellare Ataxie mit Katarakt und Oligophrenie. *Z Kinderheilkd* 1962; 87: 348–55.
- Munro S, Pelham HR. An Hsp70-like protein in the ER: identity with the 78 kd glucose-regulated protein and immunoglobulin heavy chain binding protein. *Cell* 1986; 46: 291–300.
- Muntoni F, Torelli S, Wells DJ, Brown SC. Muscular dystrophies due to glycosylation defects: diagnosis and therapeutic strategies. *Curr Opin Neurol* 2011; 24: 437–42.
- Riazuddin SA, Amiri-Kordestani L, Kaul H, Butt T, Jiao X, Riazuddin S, et al. Novel SIL1 mutations in consanguineous Pakistani families mapping to chromosomes 5q31. *Mol Vis* 2009; 15: 1050–6.
- Schapira AH. Mitochondrial disease. *Lancet* 2006; 368: 70–82.
- Schurig V, Van Orman A, Bowen P. Nonprogressive cerebellar disorder with mental retardation and autosomal recessive inheritance in Hutterites. *Am J Med Genet* 1981; 9: 43–53.
- Senderek J, Krieger M, Stendel C, Bergmann C, Moser M, Breitbach-Faller N, et al. Mutations in SIL1 cause Marinesco-Sjögren syndrome, a cerebellar ataxia with cataract and myopathy. *Nat Genet* 2005; 37: 1312–4.
- Sewry CA, Voit T, Dubowitz V. Myopathy with unique ultrastructural feature in Marinesco-Sjögren syndrome. *Ann Neurol* 1988; 24: 576–80.
- Sjögren T. Hereditary congenital spinocerebellar ataxia accompanied by congenital cataract and oligophrenia. *Confin Neurol* 1947; 10: 293–308.
- Skre H, Berg K. Linkage studies on Marinesco-Sjögren syndrome and hypergonadotropic hypogonadism. *Clin Genet* 1977; 11: 57–66.
- Takahata T, Yamada K, Yamada Y, Ono S, Kinoshita A, Matsuzaka T, et al. Novel mutations in the SIL1 gene in a Japanese pedigree with the Marinesco-Sjögren syndrome. *J Hum Genet* 2010; 55: 142–6.
- Terracciano A, Renaldo F, Zanni G, D'Amico A, Pastore A, Barresi S, et al. The use of muscle biopsy in the diagnosis of undefined ataxia with cerebellar atrophy in children. *Eur J Paediatr Neurol* 2012; 16: 248–56.
- Todorov A. Marinesco-Sjögren syndrome. 1st anatomico-clinical study. *J Genet Hum* 1965; 14: 197–233.
- Tohda H, Oikawa A, Kudo T, Tachibana T. A greatly simplified method of establishing B-lymphoblastoid cell lines. *Cancer Res* 1978; 38: 3560–2.
- Tyson JR, Stirling CJ. LHS1 and SIL1 provide a luminal function that is essential for protein translocation into the endoplasmic reticulum. *EMBO J* 2000; 19: 6440–52.
- Van Bogaert L, Scherer HJ, Epstein E. Une forme cérébrale de la cholestérose généralisée. Paris: Masson et Cie; 1937.
- Varon R, Gooding R, Steglich C, Marns L, Tang H, Angelicheva D, et al. Partial deficiency of the C-terminal-domain phosphatase of RNA polymerase II is associated with congenital cataracts facial dysmorphism neuropathy syndrome. *Nat Genet* 2003; 35: 185–9.
- Weis J, Schröder JM. Adult polyglucosan body myopathy with subclinical peripheral neuropathy: case report and review of diseases associated with polyglucosan body accumulation. *Clin Neuropathol* 1988; 7: 271–9.
- Weis J, Schröder JM. Differential effects of nerve, muscle, and fat tissue on regenerating nerve fibers *in vivo*. *Muscle Nerve* 1989; 12: 723–34.
- Wilke K, Duman B, Horst J. Diagnosis of haploidy and triploidy based on measurement of gene copy number by real-time PCR. *Hum Mutat* 2000; 16: 431–6.
- Zhao L, Longo-Guess C, Harris BS, Lee JW, Ackerman SL. Protein accumulation and neurodegeneration in the woozy mutant mouse is caused by disruption of SIL1, a cochaperone of BiP. *Nat Genet* 2005; 37: 974–9.
- Zhao L, Rosales C, Seburn K, Ron D, Ackerman SL. Alteration of the unfolded protein response modifies neurodegeneration in a mouse model of Marinesco-Sjögren syndrome. *Hum Mol Genet* 2010; 19: 25–35.
- Ziv Y, Frydman M, Lange E, Zelnik N, Rotman G, Julier C, et al. Ataxia-telangiectasia: linkage analysis in highly inbred Arab and Druze families and differentiation from an ataxia-microcephaly-cataract syndrome. *Hum Genet* 1992; 88: 619–26.